QUASI-INTERCHANGE MODES AND SAWTEETH

L.E. SUGIYAMA
Laboratory for Nuclear Science, Massachusetts Institute of Technology
Cambridge MA, USA
Email: sugiyama@mit.edu

L.Q. XU
Institute of Plasma Physics, CAS
Hefei, China

M. OKABAYASHI
Princeton Plasma Physics Laboratory
Princeton NJ, USA

Abstract

In magnetically confined fusion burning plasmas like tokamaks, high central temperature and current maximize the fusion reactivity, but can also depress the central magnetic safety factor q. If q_o falls to unity or below, a high pressure gradient can destabilize $m/n = 1/1$ sawtooth crashes. In central regions with $q \simeq 1$ and low magnetic shear, nearly ideal quasi-interchange (QI) instabilities, driven by interchange flows across the magnetic field instead of by magnetic reconnection, can produce complete central sawtooth crashes. Numerical simulation of an ITER-shape plasma with the extended MHD code M3D shows that QI modes can have unique properties. They can be fundamentally nonlinear, with multiple toroidal harmonics n at small amplitude, where the higher $m = n > 1$ harmonics align inside $q = 1$ to maximize the radial displacement of the 1/1 mode. Like the 1/1 internal kink sawtooth, the final crash that flattens the central temperature is significantly faster than the earlier instability, nearly ideal, and expels plasma to well outside $q = 1$. The simulations match detailed experimental observations of QI sawteeth and reproduce the characteristic differences with internal kink sawteeth. The final fast crashes also share basic features with the fast central crashes seen in resistive double tearing modes at $q = 2$ or 3. They suggest a common nonlinear trigger, an interchange instability driven by the large normal magnetic curvature that is produced when the original MHD instability grows to sufficiently large amplitude that it creates narrow, highly localized poloidal bulges in the magnetic field. The nonlinearly driven normal curvature interchange may be an important instability in magnetically confined plasmas. It may also be more unstable in fusion burning plasmas, at higher central temperatures and pressure gradients.

1. INTRODUCTION

In fusion tokamaks, high centrally peaked temperatures and plasma currents increase the fusion reactivity, but also depress the central magnetic safety factor q, often down to unity or below, destabilizing $m = n = 1$ MHD instabilities that cause periodic sawtooth crashes that flatten the temperature and current density over a radius larger than $q = 1$. At sufficiently low magnetic axis values $q_o < 1$, the 1/1 internal kink with magnetic reconnection is unstable, but for q_o near unity at low magnetic shear $(1/q)(dq/dr) \ll 1$, the strongest instabilities are nearly ideal quasi-interchange (QI) modes dominated by flows across the magnetic field [1,2].

Numerical simulation of an ITER-shaped DIII-D discharge with the 3D extended MHD code M3D [3,4] shows[5] that QI modes can drive an MHD sawtooth crash that completely flattens the central temperature and current density. It reproduces the characteristic QI crash properties and the differences with the internal kink seen in detailed experimental observations in DIII-D[6] and early JET [7]. Subsequent experimental observation of QI crashes in related DIII-D plasmas [8] show similar behavior. They also support a 1/1 mode magnetic well stability criterion [6,9] that includes the effect of flux surface shaping (ellipticity and triangularity), beta, and q. The criterion helps explain why the early theoretical analyses [10] and simulations [11] in circular plasmas predicted QI mode saturation short of a complete crash and why the $q \simeq 1$ $m = n$ QI-like modes observed in KSTAR [12] and other plasmas with strong central ellipticity but weak triangularity required local heating or current drive.

The final fast sawtooth crash of the $q = 1$ QI sawtooth has important similarities to other fast central crashes and suggests a possible common trigger. Sec. 2 discusses the QI sawtooth and its fast crash and compares it two other instabilities, the $q = 1$ internal kink sawtooth and the $q > 1$ double tearing mode (DTM) crash. Sec. 3 shows that an interchange mode destabilized by a strong normal magnetic curvature, can easily develop when an equilibrium MHD instability grows to large amplitude and generates region(s) of localized strong poloidal curvature, has properties consistent with the observed fast crash. Sec. 4 is a summary.

2. FAST CRASHES

2.1 Quasi-Interchange Sawtooth

Sawteeth caused by quasi-interchange (QI) modes in central $q \simeq 1$ regions have been studied for many years [1,2,7,10], but experimentally it has often difficult to distinguish them from internal kink sawteeth. Interest in QI instabilities has revived recently and more varieties have been observed, as it has been recognized that fusion plasmas with low magnetic shear central regions with $q \simeq 1$ offer possible advantages for fusion burning.

A recent numerical study of a DIII-D plasma with ITER shape and $q_o \simeq 0.95$ [5] finds new QI properties in shaped, high beta plasmas. The central QI instability is intrinsically nonlinear, with multiple toroidal harmonics at small amplitude, dominated by $n = 1$ and 2 at comparable magnitudes, that grow coherently together over many e-folding times. Inside $q \leq 1$, the $m = n$ harmonics align to maximize the radial displacement of the 1/1 mode. The individual harmonics resemble theoretically expected linear quasi-interchange modes [1,2]. The higher $m = n$ components inside $q = 1$ concentrate closer to the outer $q = 1$ surface where destabilizing imbalance in the interchange magnetic well effects are cancelled less completely, than on more central flux surfaces.

The mode is driven by the quasi-interchange flows across the low shear magnetic field. As expected, the mode is nearly ideal. The entire evolution, from the formation of the small amplitude perturbation, to the QI crash of the central temperature and the subsequent temperature flattening, followed by the current density flattening, is nearly independent of resistivity for Lundquist numbers $S = 10^6$ to 10^8. There is no resonant magnetic reconnection.

For the quasi-interchange mode, the degree of magnetic shear is relative to the strength of the force driving the interchange flows. In this case, as in other plasmas that have significant central $q \simeq 1$ regions, the shear remains rather weak for some distance outside $q = 1$. (The $q = 1$ radius is at approximately $r/a = 0.3$ on the outer midplane, and $q = 3/2$ is rather far out at about $r/a = 0.6$, for $q_{95} = 4.2$.) The exterior shear is smaller than in most higher shear plasmas with lower axis q_o. The radial extent of the central mode convective flow cells and the distance outside $q = 1$ that the crash can expel the central plasma are relatively large.

While the temperature appears to follow the magnetic field before the crash, in reality both move due to the flow. Simulation with M3D [5] shows that the mode develops into a fast final crash of the central temperature, where the plasma is expelled in narrow poloidal flow channels. Unlike the internal kink sawtooth, where the outflow is controlled by the single magnetic reconnection point, the QI outflow splits poloidally into two channels about ± 60 degrees poloidally on either side of the original mode direction (Fig. 1(d)). These channels are spread apart and narrowed due to nonlinear backflow along the center of the original outflow direction from convective cells that form in the gap. The process is shown in Fig 1, which shows an expanded cross section of the central plasma. The background color shows the total MHD temperature T. Note the extent of the original convective flow cells well outside q=1, even in the small amplitude mode (a). They extend further as the mode grows.

Figure 2 shows magnetic puncture plots for the growing nonlinear mode of Fig. 1 over most of the plasma cross section. Magnetic islands develop from very small perturbations of the field in the low magnetic shear region carried by the flows, without resonant reconnection. Comparison with Fig. 1 shows that the magnetic boundaries follow the flow contours rather than the smoother T contours. By the crash time $t = 584.8$ in Fig. 2(c), the magnetic structure has also narrowed into two channels near $q = 1$.

The QI sawtooth crash is not observed in the actual plasma, because the temperature and pressure profiles are actually hollow over $q \leq 1$, rather than weakly peaked as in the EFIT equilibrium reconstruction used for the simulation. However, QI sawteeth are observed in other similar plasmas, reported at this conference [8].

The post-crash plasma has central $q = 1$ with even lower magnetic shear. It also naturally develops QI-type modes with multiple harmonics, mainly $n = 1$ and 2. The $n = 2$ harmonic, in addition to $n = 1$, also appears in the actual plasma, as well as in other shaped QI sawtooth plasmas, including the DIII-D QI/IK sawtooth study [6] and early JET sawteeth ([7], detailed SXR picture in [13]).

2.2 Internal Kink Sawtooth

The simulation results show that the final fast crash of the $q = 1$ QI sawtooth has some basic similarities with the fast crash of the $q = 1$ internal kink sawtooth at lower $q_o < 1$ and higher magnetic shear.

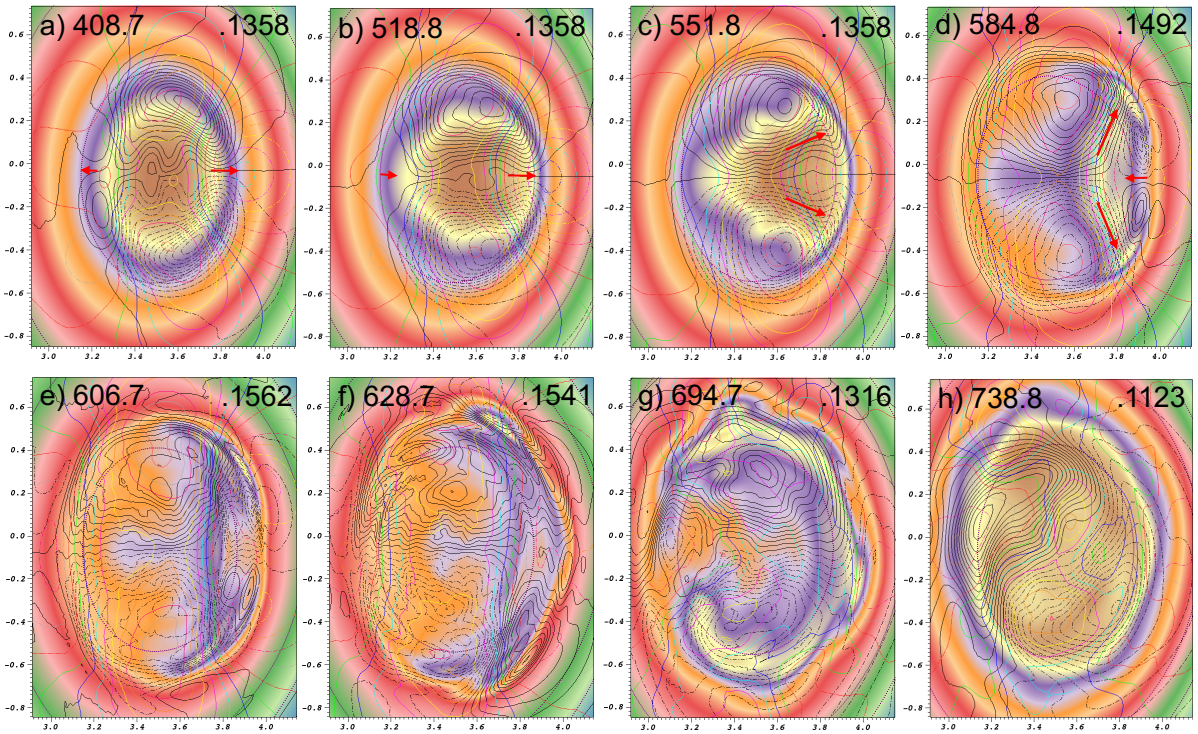

Figure 1. QI mode and start of crash. a) low amplitude mode with comparable $n = 1$ and 2, b) increasing amplitude where $n = 1$ begins to increase relative to $n = 2$, c) outflow begins to separate into two channels d) narrow, strong outflow velocity channels have partially expelled plasma and temperature to well outside $q = 1$. The outflow is nearly finished by $t = 607$. Background solid color shows total temperature T (close to the pressure). Red arrows show flow directions (not to scale). Black lines show equi-spaced contours of poloidal velocity stream function U, (positive values are solid lines, negative dashed). Multicolor lines are contours of perturbed magnetic flux $\tilde{\psi}$. Variables scaled to instantaneous maximum values over the plasma; maximum temperature values at upper right in each frame. Concentric ellipses (dotted) show $q(\psi) = 1$, 1.5, 2, and 3 surfaces. ($q = 1$ in dark purple band; q=3/2 at outer boundary of red band)

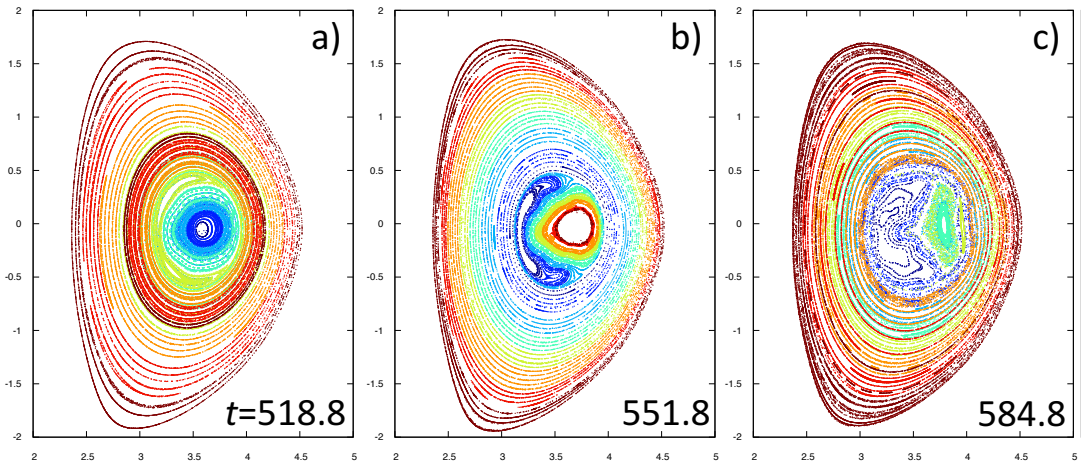

Figure 2. Magnetic puncture plots for the QI crash of Fig. 1.

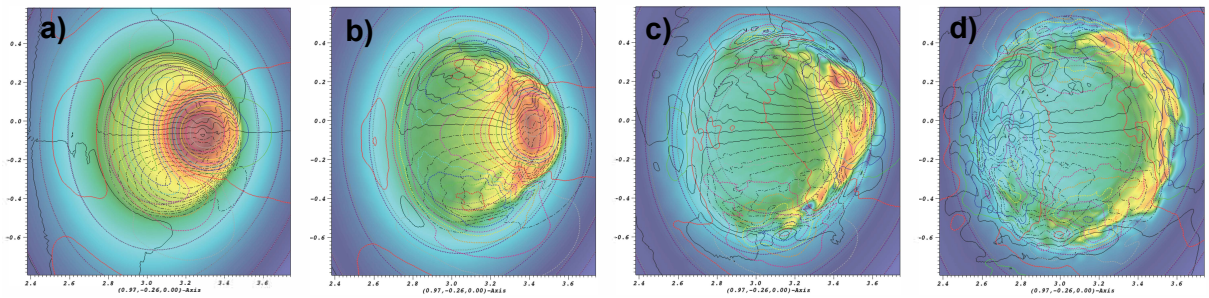

Figure 3. Later internal kink sawtooth crash and loss of the hot core at times a) $t = 1058.1$, b) 1071.5, c) 1077.7, and d) 1084.3τ_A. a) Hot core and island. c) Final crash outflow (black contours) directly through the center of the remaining hot core at $t = 1077.7$ (core has rotated slightly counter-clockwise from previous time) creates d) Hot layer forms a partial annulus outside $q = 1$, that is equilibrating along field lines. Background solid color shows total pressure p (close to T). Black lines show equi-spaced contours of poloidal stream function U, multicolor lines the contours of perturbed magnetic flux $\tilde{\psi}$ (positive values are solid lines, negative dashed). Variables scaled to instantaneous maximum values over the plasma. Concentric ellipses (dotted) show $q(\psi) = 1$, 1.5, 2, and 3 surfaces. From M3D simulation of $S = 10^7$ higher resolution case [15].

Experimentally, a final fast crash occurs in the $q = 1$ internal kink mode sawtooth when the contact region of the hot central core with the $q \simeq 1$ surface becomes highly localized poloidally Some degree of toroidal localization $n > 1$ also develops, but is harder to measure accurately. Without strong localization, the crash is slow or non-existent. Electron Cyclotron Emission Imaging (ECEI) [14] shows that the final rapid expulsion of the electron temperature from $q < 1$ occurs through a poloidally narrow, radially directed channel that extends beyond $q = 1$. The expelled temperature equilibrates along field lines to form a hot annulus outside $q = 1$. This behavior is reproduced by MHD numerical simulations [15]. Nozzle-like expulsion and a final hot annulus outside $q = 1$ are seen in the QI sawteeth, in M3D simulations and in the early JET sawteeth that originally inspired the idea of a QI sawtooth crash.

Simulation[15] with M3D showed that the IK sawtooth followed the expected resistive development of a 1/1 magnetic island and approximately circular hot core inside $q = 1$. The core shrunk steadily until small, when a sudden fast crash The time history of the harmonics for several cases (Figs. 1–2 in [15]) showed that the mode first grew at a constant exponential linear rate. As it became nonlinear, the velocity began to grow at a faster steadily accelerating rate up to the final crash. The poloidal magnetic flux continued to grow at the constant exponential rate until immediately before the final crash, when the hotter temperature was completely lost from inside $q = 1$. The approach to the crash was independent of resistivity. The time-histories at different resistivities between Lundquist numbers $S = 10^6$–10^8 overlaid almost exactly for the growing mode preceding the final crash, even though the initial linear growth rates were quite different. (The history plotted volume integrals of the n=1 harmonics over the plasma. Immediately before the final crash the higher harmonics make a larger contribution.)

An example crash is shown in Fig. 2. The background color scheme differs from Fig 1, but black contours still represent the poloidal velocity stream function. Note the compressed, narrow flow channel in the poloidal stream function U at the penultimate time (c), $t = 1077.7$ as the hot core is being lost.

2.3 Double Tearing Mode

The Double Tearing Mode (DTM) [16] can also generate strong fast crashes of pressure and temperature [17] in two types of crashes, on and off the central magnetic axis. The crashes appear in RMHD as well as MHD simulations.

In tokamaks, the DTM can grow in a non-monotonic q profile, where two rational magnetic surfaces, in tokamaks typically $q_s = 2$ or 3, surround a somewhat lower-q region. Magnetic island chains form at each q_s-surface, linked by the radial displacement so that their X- and O- points anti-align. The outer islands typically grow larger first and squeeze the inner q_s islands into poloidally narrowing regions. The inner islands are forced to extend radially and may interact (reconnect) with the inner core inside q_s. They also extend outward toward the outer q_s surface and can come to resemble radial "spokes" on a wheel. They contact the outer q_s surface at the X-points of the outer islands, separating the outer islands but preserving their contact at the X-points, where they continue to reconnect and grow. At first, the inner islands have little interaction with the outer X-points. The narrowing islands gradually develop an outward radial flow aligned along their length. If the poloidal width of the inner islands there becomes sufficiently narrow, a sudden fast crash through their outer tips can flatten the pressure over the entire annulus

$q < q_s$ annulus. The crash is nearly independent of resistivity. If the inner q_s surface is also sufficiently close to the magnetic axis and the instability strong enough, the crash can extend through the axis $q_o > q_s$, an "on-axis" crash. If the inner islands do not narrow sufficiently at their outer X-points, no fast crash occurs (in RMHD and MHD simulation [18]). The critical magnetic curvature near the X-point (poloidal width) is similar to that of the QI $q = 1$ fast crash.

The multiple, well-separated inner spokes of the DTM have some resemblance to the two outflow legs of the QI sawtooth core and the fast crash appears to be a similar cross-field expulsion. There is one important difference, however. The basic DTM is a resonant resistive tearing instability at $q = q_s$. Reconnection drives the growth of the outer island at the outer q_s surface and sometimes, reconnection of the inner islands with the central magnetic core. (The core reconnection requires that the inner magnetic X-points of the inner islands shift poloidal location.)

The DTM sawtooth progresses through three stages. The first two are similar to resistive magnetic island growth – linear exponential growth followed by a slower nonlinear Rutherford exponential growth with $\gamma \sim \eta$. Then a nearly ideal fast crash suddenly grows out of the Rutherford phase, with an accelerating growth rate that is much faster than exponential. The outer X-point changes steadily during the Rutherford phase, but its characteristics change in the fast crash. The outer islands continue to grow steadily until the final fast crash removes the driving factors, but the growth rate is much slower than crash.

The inner islands have only weak reconnection at the outer X-points because the radial flow into the X-point is weak and their radial gradients at their tip are also weak, similar to the 1/1 $q = 1$ QI mode.

3. NORMAL CURVATURE INTERCHANGE

Because of the large separation of scales, the trigger for the nonlinear normal curvature interchange can be seen from the free energy of an instability in a slowly varying background plasma that describes the growth of the initial MHD instability. The interchange term in the free energy can arise from two potentially independent sources the magnetic island configuration as reflected in the local perpendicular current density term $\mathbf{J} \times \mathbf{B}$, or the pressure gradient ∇p. These are equivalent in a static or slowly evolving plasma, but decouple in the presence of background plasma flow. The explicit pressure-gradient term is also removed by incompressibility, but in this limit it can be replaced by the magnetic term.

The following discussion summarizes the basic relations, discussed in a separate paper.

The Frieman-Rotenberg equations for a small MHD perturbation can be used to take into account background flow, but in the fast crash the background velocity and its effects are small compared to the growth rate of the new mode. This means that the free energy terms involving the background velocity, except perhaps for convection, can be dropped relative to the other mode terms. The perturbation is assumed to have a temporal/spatial separation of variables, $\hat{f}(\mathbf{x}, t) = \tilde{f}(\mathbf{x}) \exp(\gamma t)$. The growth rate γ can be complex, but for the fast crash, it is mostly real. The plasma displacement $\boldsymbol{\xi}$ is defined in terms of the Lagrangian velocity by $\mathbf{v}(\mathbf{r}^0 + \boldsymbol{\xi}, t) = (D\mathbf{r}^0/Dt) + (D\boldsymbol{\xi}^0/Dt) = \mathbf{v}^0 + \mathbf{v}^0 \cdot \nabla^0 \boldsymbol{\xi} + (\partial \boldsymbol{\xi}/\partial t)$, where the superscript 0 designates quantities that describe the unperturbed flow. In the following equations, it is dropped from all the background plasma variables and operators.

The linearized equations for the momentum, pressure, and combined Faraday's and Ohm's laws become

$$\rho\gamma\boldsymbol{\xi} = -\tilde{\mathbf{B}} \times \mathbf{J} + \tilde{\mathbf{J}} \times \mathbf{B} - \nabla\tilde{p} - \rho(\mathbf{v} \cdot \nabla)\boldsymbol{\xi} - \rho(\boldsymbol{\xi} \cdot \nabla)\mathbf{v} \quad (1)$$

$$\tilde{p} = -\boldsymbol{\xi} \cdot \nabla p - \Gamma p \nabla \cdot \boldsymbol{\xi} \quad (2)$$

$$\tilde{\mathbf{B}} = \nabla \times (\boldsymbol{\xi} \times \mathbf{B}) + (\eta/\gamma)\nabla^2 \tilde{\mathbf{B}}, \quad (3)$$

where Γ is the ratio of specific heats. In $\tilde{p}$ and $\tilde{\mathbf{B}}$, the explicit background velocity terms have been dropped. The electrical resistivity $\eta = \eta(T_e)$ is assumed to be small compared to γ, so that the last term in Eq. (3) is dropped in δW. The thermal conductivity terms in the pressure equation (2) have also been dropped, since typically they have only small effects on ordinary MHD perturbations and the fast crash is even faster.

The Frieman-Rotenberg force operator $\mathbf{G}(\boldsymbol{\xi})$ satisfies

$$\mathbf{G}(\boldsymbol{\xi}) = 2\rho(\mathbf{v}\cdot\nabla)\frac{\partial\boldsymbol{\xi}}{\partial t} + \rho\frac{\partial^2\boldsymbol{\xi}}{\partial t^2} \tag{4}$$

$$\mathbf{G}(\boldsymbol{\xi}) = \mathbf{F}(\boldsymbol{\xi}) + \nabla\cdot\big(\boldsymbol{\xi}\rho(\mathbf{v}\cdot\nabla)\mathbf{v} - \rho\mathbf{v}(\mathbf{v}\cdot\nabla)\boldsymbol{\xi}\big) \tag{5}$$

$$\mathbf{F}(\boldsymbol{\xi}) = -\mathbf{B}\times(\nabla\times\tilde{\mathbf{B}}) + \mathbf{J}\times\tilde{\mathbf{B}} + \nabla\big[\Gamma p(\nabla\cdot\boldsymbol{\xi}) + \boldsymbol{\xi}\cdot\nabla p\big], \tag{6}$$

where $\mathbf{F}$ is the force operator for a static plasma. The free energy $\delta W \equiv (1/2)\int d\tau\,\rho\gamma^2\boldsymbol{\xi}^2$ is obtained by dotting $\boldsymbol{\xi}$ into Eq. 4 and taking the volume integral over the plasma, as $2\delta W + \gamma\int d\tau\,\rho\,\mathbf{v}\cdot\nabla\xi^2 = \int d\tau\,\boldsymbol{\xi}\cdot\mathbf{G}(\boldsymbol{\xi})$. Writing terms in the form $\nabla\cdot\mathbf{C}$ and converting volume integrals to surface integrals $\int d\mathbf{S}\cdot\mathbf{C}$ over the boundary surface and assuming that either the normal displacement or $\mathbf{C}\cdot d\mathbf{S}$ there is zero,

$$\int d\tau\,\boldsymbol{\xi}\cdot\mathbf{G}(\boldsymbol{\xi}) = \int d\tau\left\{\tilde{\mathbf{B}}^2 + \mathbf{J}\cdot(\boldsymbol{\xi}\times\tilde{\mathbf{B}}) + (\boldsymbol{\xi}\cdot\nabla p)(\nabla\cdot\boldsymbol{\xi}) + \Gamma p(\nabla\cdot\boldsymbol{\xi})^2 - \rho(\mathbf{v}\cdot\nabla)\mathbf{v}\cdot(\boldsymbol{\xi}\cdot\nabla)\boldsymbol{\xi} + \rho\big((\mathbf{v}\cdot\nabla)\boldsymbol{\xi}\big)^2\right\}. \tag{7}$$

The second line represents the static background contribution $\int d\tau\,\boldsymbol{\xi}\cdot\mathbf{F}(\boldsymbol{\xi})$ from Eq. (6) and the third line the background flow effects from Eq. (5). The squared terms are always stabilizing.

The current term $\mathbf{J}\cdot(\boldsymbol{\xi}\times\tilde{\mathbf{B}})$ can be split into parallel and perpendicular currents, $\mathbf{J}\cdot(\boldsymbol{\xi}\times\tilde{\mathbf{B}}) = (J_\parallel/B)(\boldsymbol{\xi}\times\mathbf{B})\cdot\tilde{\mathbf{B}} - (1/B^2)\boldsymbol{\xi}\cdot[(\mathbf{J}\times\mathbf{B})(\mathbf{B}\cdot\tilde{\mathbf{B}}) - \mathbf{B}((\mathbf{J}\times\mathbf{B})\cdot\tilde{\mathbf{B}})]$, where $\mathbf{J}_\perp \equiv (1/B^2)(\mathbf{B}\times(\mathbf{J}\times\mathbf{B}))$ and $J_\parallel \equiv \mathbf{J}\cdot\mathbf{B}/B$. The second, perpendicular current piece can be evaluated in terms of the magnetic curvature $\boldsymbol{\kappa} \equiv \big(\hat{\boldsymbol{b}}\cdot\nabla\big)\hat{\boldsymbol{b}}$ and the parallel perturbed field $\mathbf{B}\cdot\tilde{\mathbf{B}}$ from Eq. (3).

In a magnetically confined static-background toroidal plasma with finite pressure gradient $\nabla p = \mathbf{J}\times\mathbf{B}$ and compressibility $\nabla\cdot\boldsymbol{\xi}$, the free energy is [20]

$$\int d\tau\,\boldsymbol{\xi}\cdot\mathbf{G}(\boldsymbol{\xi}) = \int d\tau\left\{\left|\tilde{\mathbf{B}} - \frac{\boldsymbol{\xi}\cdot\nabla p}{B^2}\mathbf{B}\right|^2 - \frac{J_\parallel}{B}(\boldsymbol{\xi}\times\mathbf{B})\cdot\tilde{\mathbf{B}} - 2(\boldsymbol{\xi}\cdot\nabla p)(\boldsymbol{\xi}\cdot\boldsymbol{\kappa}) + \Gamma p|\nabla\cdot\boldsymbol{\xi}|^2\right\}, \tag{8}$$

where all occurrences of $\mathbf{J}\times\mathbf{B}$ have been replaced by ∇p. The first, squared term on the right, containing $\tilde{\mathbf{B}}^2$, represents the stabilizing effects of magnetic field line stretching, where the $J_\perp$ terms proportional to $(\mathbf{B}\cdot\tilde{\mathbf{B}})$ have been added. The $J_\parallel$ term represents the internal kink. The third term is usual expression for the interchange mode free energy. It arises from the compressional pressure gradient term $(\boldsymbol{\xi}\cdot\nabla p)(\nabla\cdot\boldsymbol{\xi})$ in Eq. (7), when $\nabla\cdot\boldsymbol{\xi}$ is expressed in terms of $\mathbf{B}\cdot\tilde{\mathbf{B}}$ and $\boldsymbol{\kappa}$. The last term is the stabilizing compressional term. The remaining terms supply the cross term in the field line stretching.

In an incompressible plasma with flow, $\nabla\cdot\mathbf{v} = \nabla\cdot\boldsymbol{\xi} = 0$, the usual source of the interchange term, $(\boldsymbol{\xi}\cdot\nabla p)(\nabla\cdot\boldsymbol{\xi})$, vanishes. However, terms $\boldsymbol{\xi}\cdot\mathbf{J}\times\mathbf{B}$ can be added and subtracted from $\tilde{\mathbf{B}}^2$ to obtain

$$\int d\tau\left\{\left|\tilde{\mathbf{B}} - \frac{\boldsymbol{\xi}\cdot(\mathbf{J}\times\mathbf{B})}{B^2}\mathbf{B}\right|^2 - \frac{J_\parallel}{B}\boldsymbol{\xi}\times\mathbf{B}\cdot\tilde{\mathbf{B}} - 2\big(\boldsymbol{\xi}\cdot(\mathbf{J}\times\mathbf{B})\big)\big(\boldsymbol{\xi}\cdot\boldsymbol{\kappa}\big) - \rho(\mathbf{v}\cdot\nabla)\mathbf{v}\cdot(\boldsymbol{\xi}\cdot\nabla)\boldsymbol{\xi} + \rho\big((\mathbf{v}\cdot\nabla)\boldsymbol{\xi}\big)^2\right\}. \tag{9}$$

This describes RMHD plasmas and is equivalent to the usual interchange if $\mathbf{J}\times\mathbf{B} \equiv \nabla p$.

A general compressible solution that keeps the ∇p and $\mathbf{J}\times\mathbf{B}$ terms separate is

$$\begin{aligned}\int d\tau\;&\left\{\left|\tilde{\mathbf{B}} - \frac{\boldsymbol{\xi}\cdot(\mathbf{J}\times\mathbf{B}+\nabla p)}{2B^2}\mathbf{B}\right|^2 - \frac{J_\parallel}{B}(\boldsymbol{\xi}\times\mathbf{B})\cdot\tilde{\mathbf{B}} - 2(\boldsymbol{\xi}\cdot\nabla p)(\boldsymbol{\xi}\cdot\boldsymbol{\kappa}) + \Gamma p|\nabla\cdot\boldsymbol{\xi}|^2\right.\\ &- \rho(\mathbf{v}\cdot\nabla)\mathbf{v}\cdot(\boldsymbol{\xi}\cdot\nabla)\boldsymbol{\xi} + \rho\big((\mathbf{v}\cdot\nabla)\boldsymbol{\xi}\big)^2\\ &\left.- \left[\frac{\boldsymbol{\xi}\cdot(\mathbf{J}\times\mathbf{B}+\nabla p)}{2B^2}\mathbf{B}\right]^2 + \frac{(\boldsymbol{\xi}\cdot\nabla p)(\boldsymbol{\xi}\cdot(\mathbf{J}\times\mathbf{B}))}{B^2} + \frac{(\boldsymbol{\xi}\cdot\nabla p)}{B^4}\mathbf{B}\cdot\nabla[(\boldsymbol{\xi}\cdot\mathbf{B})B^2] + \tilde{\mathbf{B}}\cdot\frac{(\mathbf{J}\times\mathbf{B})}{B^2}(\boldsymbol{\xi}\cdot\mathbf{B})\right\}.\end{aligned}$$

Again, $\mathbf{v}$ terms apart from the Frieman-Rotenberg convection have been dropped. The extra terms on the last line are small in general for the interchange, because they each contain one component of $\boldsymbol{\xi}$ parallel and one perpendicular to $\mathbf{B}$.

The normal curvature interchange instability is much stronger than the typical interchange in the equilibrium plasma, even though both come from the $-2(\boldsymbol{\xi}\cdot\nabla p)(\boldsymbol{\xi}\cdot\boldsymbol{\kappa})$ term. In a typical toroidal equilibrium such as a

tokamak, the magnetic curvature $\boldsymbol{\kappa}$ is primarily geodesic and lies in the magnetic flux surface. Its large size forces the mode displacement $\boldsymbol{\xi}$ to also be primarily geodesic, with only a small normal component radial to the flux surface (cf. [20]). The main interchange effects on the plasma come from the normal displacement.

For the normal curvature interchange, the strong local poloidal variation in the curvature at the beginning of the fast crash creates a dominant normal (radial) component. The main active displacement is also radial. Even if the pressure gradient is relatively modest, the net instability is much stronger. In the examples here, the poloidal variation has equivalent poloidal harmonic $m \sim 6$ or more, much larger than the $m \lesssim 1$ of the equilibrium mode, even without taking into account that the radial displacement is strongly reduced relative to the total (by a few orders in a small parameter expansion such as the inverse aspect ratio [20]). It is not surprising that a sudden fast-growing MHD instability appears once the normal curvature begins to dominate the other terms.

4. SUMMARY

In toroidal fusion plasmas, a different type of fast growing, highly localized, and nearly ideal interchange instability can appear, driven by a large normal magnetic curvature that is produced by local poloidal bulging of the magnetic field. It has an accelerating, faster-than-exponential growth rate. It can cause a rapid crash of the temperature and plasma in the interior plasma region as they are carried out through one or more localized radial flow channels. The required destabilizing magnetic curvature can easily be produced by certain conventional MHD instabilities, if they are able to grow to a sufficiently large nonlinear amplitude that produces a strong distortion of the total magnetic flux surfaces. The type of the initial instability is less important than its ultimate large size and distorting effects, although the analysis is complicated by the fact that the original instability can continue to grow until the final crash. Examples include the $q = 1$ 1/1 resistive internal kink and the nearly ideal $m = n$ quasi-interchange mode, and also double tearing modes over the annulus between two $q = q_s = m/n$ surfaces, typically $q_s = 2$ or 3. The normal curvature instability appears in RMHD and MHD simulations. Its trigger appears in the free energy of an interchange-type instability growing on a slowly evolving, non-axisymmetric background and is much larger than the free energy of interchange instabilities in typical magnetically confined equilibria. In $q = 1$ sawteeth and in DTMs located sufficiently close to the magnetic axis, the final crash affects the entire central plasma inside the outer resonant surface. In fusion tokamak examples, the poloidal width of the curved field at the onset of the fast crash has roughly the same size in all three cases, roughly $m \sim 6$. The instability should appear in other magnetically confined plasmas where the magnetic curvature can be similarly changed.

ACKNOWLEDGEMENTS

Work partially supported by the US Department of Energy under DE-SC0007883, DE- FG02-04ER54761 and DE-FC02-04ER54698, and by the China Scholarship Council. Simulations run at NERSC.

REFERENCES

[1] HASTIE, R.J., HENDER, T.C., CARRERAS, B.A., CHARLTON, L.A., HOLMES, J.A., Stability of ideal and resistive internal kink modes in toroidal geometry, Phys. Fluids **30** (1987) 1756.

[2] WAELBROECK, F.L., HAZELTINE, R.D., Stability of low-shear tokamaks, Phys. Fluids **31** (1988) 1217.

[3] Park, W., BELOVA, E.V., FU, G.Y., TANG, X.Z., STRAUSS, H.R., SUGIYAMA, L.E, Plasma Simulation Studies Using Multi-Level Simulation Models, Phys. Plasmas **6** (1999) 1796.

[4] SUGIYAMA, L., PARK, W., A nonlinear two-fluid model for toroidal plasmas, Phys. Plasmas **7** (2000) 4664.

[5] SUGIYAMA, L.E., XU, L.Q., OKABAYASHI, M.O., Quasi-interchange modes and sawteeth, submitted to Phys. Plasmas (2020).

[6] LAZARUS, E.A., LUCE, T.C., AUSTIN, M.E., et al., Sawtooth oscillations in shaped plasmas, Erratum Phys. Plasmas **15** (2008) 129901.

[7] EDWARDS, A.W., CAMPBELL, D.J., ENGELHARDT, W.W., et al., Rapid Collapse of a plasma sawtooth oscillation in the JET tokamak, Phys. Rev. Lett. **57** (1986) 210.

[8] OKABAYASHI, M., SUGIYAMA, L., BRENNAN, D.P., INOUE, S., CHRYSTAL, C., LA HAYE, R.J., STRAIT, E.J., AUSTIN, M., LOGAN, N.C., HOLCOMB, C., VICTOR, B., HANSON, J. Slowly rotating 3D field for locked mode avoidance and H-Mode recovery in DIII-D, this conference, session TH/P1.

[9] GREENE, J.M., A brief review of magnetic well, Comments Plasma Phys. Controlled Fusion **17** (1997) 389.

[10] WAELBROECK, F.L., Nonlinear growth of the quasiinterchange instability, Phys. Fluids B **1** (1989) 499.

[11] AYDEMIR, A.Y., Mechanism for rapid sawtooth crashes in tokamaks, Phys. Rev. Lett. **59** (1987) 649.

[12] CHOE, G.H., YUN, G.S., NAM, Y., LEE, W., PARK, H.K., BIERWAGE, A., DOMIER, C.W., LUHMANN JR, N.C., JEONG, J.H., BAE, Y.S., and the KSTAR TEAM, Dynamics of multiple flux tubes in sawtoothing KSTAR plasmas heated by electron cyclotron waves: I. Experimental analysis of the tube structure, Nucl. Fusion **55** (2015) 013015.

[13] HASTIE, R.J., Sawtooth instability in tokamak plasmas, Astrophys. and Space Science **256** (1998) 177.

[14] PARK, H.K., DONNÉ, LUHMANN JR. N.C., et al., and TEXTOR Team, Comparison Study of 2D Images of Temperature Fluctuations during Sawtooth Oscillation with Theoretical Models, Phys. Rev. Lett. **96** (2006) 195004.

[15] SUGIYAMA, L.E., Mode coupling and aspect ratio effects on low and high-n plasma instabilities, Nucl. Fusion **55** (2015) 073006.

[16] PRITCHETT, P.L., LEE, Y.C., DRAKE, J.F., Linear analysis of the double-tearing mode, Phys. Fluids **23** (1980) 1368.

[17] CHANG, Z., PARK, W., FREDRICKSON, E.D., et al., Off-Axis Sawteeth and Double-Tearing Reconnection in Reversed Magnetic Shear Plasmas in TFTR, Phys. Rev. Lett. **77** (1996) 3553.

[18] ISHII, Y., Long timescale plasma dynamics and explosive growth driven by the double tearing mode in reversed shear plasmas, Nucl. Fusion **43** (2003) 539-546.

[19] JOHNSON, J.L., GREENE, J.M., Resistive interchanges and the negative V" criterion, Plasma Physics **9** (1967) 611.